Molecular Cell *23*, 887–897, September 15, 2006 ©2006 Elsevier Inc. DOI 10.1016/j.molcel.2006.08.017

Chaperonin TRiC Promotes the Assembly of polyQ Expansion Proteins into Nontoxic Oligomers

Christian Behrends,[1,4] Carola A. Langer,[1,4] Raina Boteva,[3] Ulrike M. Böttcher,[1] Markus J. Stemp,[1] Gregor Schaffar,[1] Bharathi Vasudeva Rao,[1] Armin Giese,[2] Hans Kretzschmar,[2] Katja Siegers,[1] and F. Ulrich Hartl[1,*]

[1] Department of Cellular Biochemistry
Max Planck Institute of Biochemistry
Am Klopferspitz 18
D-82152 Martinsried

[2] Zentrum für Neuropathologie und Prionforschung
Ludwig-Maximilians-Universität München
Germany

[3] Radiobiology Department
National Center of Radiobiology and Radiation Protection
1756 Sofia
Bulgaria

Summary

Aberrant folding and fibrillar aggregation by polyglutamine (polyQ) expansion proteins are associated with cytotoxicity in Huntington's disease and other neurodegenerative disorders. Hsp70 chaperones have an inhibitory effect on fibril formation and can alleviate polyQ cytotoxicity. Here we show that the cytosolic chaperonin, TRiC, functions synergistically with Hsp70 in this process and is limiting in suppressing polyQ toxicity in a yeast model. In vitro reconstitution experiments revealed that TRiC, in cooperation with the Hsp70 system, promotes the assembly of polyQ-expanded fragments of huntingtin (Htt) into soluble oligomers of ~500 kDa. Similar oligomers were observed in yeast cells upon TRiC overexpression and were found to be benign, in contrast to conformationally distinct Htt oligomers of ~200 kDa, which accumulated at normal TRiC levels and correlated with inhibition of cell growth. We suggest that TRiC cooperates with the Hsp70 system as a key component in the cellular defense against amyloid-like protein misfolding.

Introduction

A subset of newly synthesized proteins in the eukaryotic cytosol requires the assistance of the Hsp70 chaperone system and the chaperonin TRiC/CCT for de novo folding (Frydman, 2001; Hartl and Hayer-Hartl, 2002). Hsp70 members, together with Hsp40 cochaperones, can interact cotranslationally with nascent polypeptide chains, protecting them against premature misfolding and aggregation, whereas TRiC acts downstream in mediating folding and oligomeric assembly. Whether these chaperones also cooperate in preventing the formation of aberrantly folded proteins associated with neurodegenerative disorders, such as Huntington's or Parkinson's disease, has remained largely unexplored.

*Correspondence: uhartl@biochem.mpg.de

[4] These authors contributed equally to this work.

Huntington's disease (HD) and several other late-onset neurodegenerative disorders are caused by expansion of polyglutamine (polyQ) repeats in otherwise unrelated disease proteins (Landles and Bates, 2004; Zoghbi and Orr, 2000). The pathogenic length of the polyQ stretch is typically greater than ~37 Q. Aberrant folding of such proteins, leading to their deposition as insoluble, fibrillar aggregates (inclusions) in the cytoplasm and nucleus of neurons, is associated with cytotoxicity resulting from interference by the misfolded proteins with various cell functions, including transcriptional regulation and proteasomal degradation (Bence et al., 2001; Sugars and Rubinsztein, 2003). In the fibrils, the polyQ sequence adopts a regular β sheet structure, possibly forming curved or triangular, parallel β sheets with ~20 Q per turn (Wetzel, 2002). Increased expression of chaperones of the heat-shock protein (Hsp) 70 family, together with various Hsp40 cofactors, has been shown to alleviate polyQ toxicity and neurodegeneration in various cellular and animal models, presumably by redirecting the aggregation process toward the formation of nonfibrillar, amorphous aggregates (Chan et al., 2000; Cummings et al., 1998; Muchowski et al., 2000; Schaffar et al., 2004; Warrick et al., 1999). This mechanism is thought to inhibit the accumulation of certain aggregation intermediates, including soluble polyQ oligomers, which may be the primary toxic agents (Arrasate et al., 2004; Schaffar et al., 2004; Wacker et al., 2004).

A recent RNA interference screen in *C. elegans* invoked the cytosolic chaperonin, TRiC, as a previously unknown modulator of polyQ aggregation (Nollen et al., 2004). TRiC is an ~900 kDa cylindrical complex with ATPase activity consisting of eight homologous subunits that are arranged in two octameric rings stacked back to back (Hartl and Hayer-Hartl, 2002; Spiess et al., 2004). Its substrates include actins, tubulins, several WD40 repeat proteins, and the von Hippel-Lindau tumor suppressor protein (VHL) (Frydman, 2001; Melville et al., 2003; Siegers et al., 2003). Unfolded proteins bind in the ring center, contacting multiple apical domains of the TRiC subunits, and are then transiently enclosed in the TRiC central cavity for folding in a process involving ATP-regulated movements of α-helical extensions of the subunits (Meyer et al., 2003). Substrates may be presented to TRiC by Hsp70 and/or the cochaperone prefoldin (Hartl and Hayer-Hartl, 2002). Moreover, TRiC appears to cooperate with Hsp70 in oligomeric protein assembly by transiently stabilizing protein subunits in assembly-competent conformations (Melville et al., 2003).

Here, we conducted a series of in vitro and in vivo experiments to explore the interaction of TRiC with polyQ-expanded fragments of huntingtin (Htt), the disease protein in HD. TRiC was found to interfere with polyQ fibril formation and proved to be limiting in suppressing polyQ toxicity in a yeast model. Remarkably, the chaperonin cooperated with Hsp70 and Hsp40 in promoting the assembly of benign Htt oligomers of ~500 kDa. This process is reminiscent of the sequential action of these

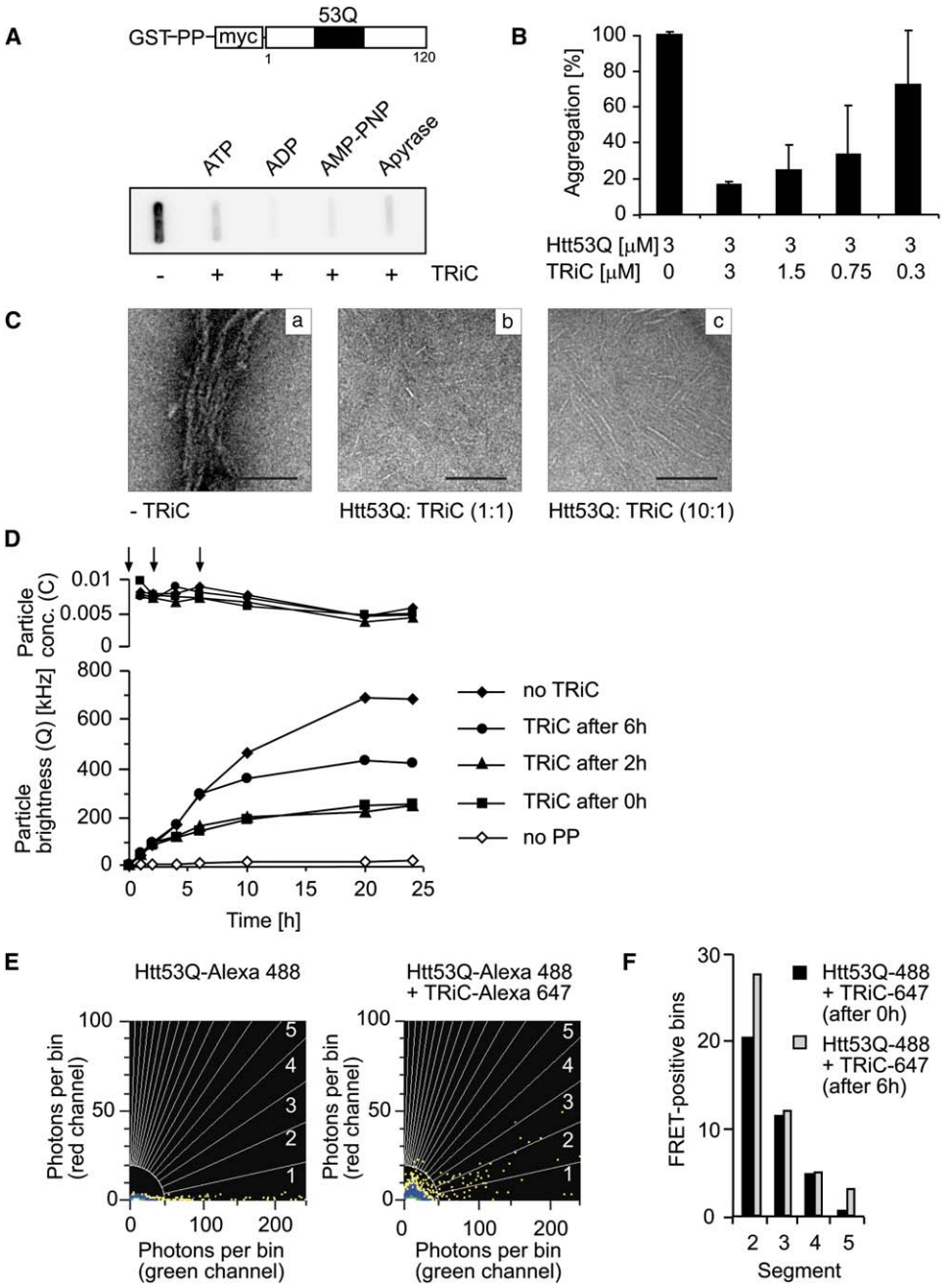

Figure 1. Inhibition of Htt53Q Aggregation by TRiC

(A) Effect of purified TRiC on formation of SDS-insoluble aggregates of myc-tagged Htt53Q exon 1 protein, monitored by filter-trap assay. Aggregation was performed at 30°C with 3 μM GST-myc-Htt53Q and 3 μM bovine TRiC either in the presence of 2 mM ATP and an ATP-regenerating system, with 2 mM ADP, 2 mM AMP-PNP, or in a nucleotide-free buffer containing 10 U/ml apyrase. $MgCl_2$ was present at 5 mM. Aggregation was initiated by addition of 2.5 U PP to cleave GST-Htt53Q and stopped after 8 hr by heating in 4% SDS/100 mM DTT (Muchowski et al., 2000). Aggregates were detected with anti-myc antibody. The GST-myc-Htt53Q construct used is shown schematically, with the numbering referring to amino acid residues of Htt exon 1.

(B) Effects of different TRiC concentrations on formation of SDS-insoluble aggregates of Htt53Q monitored by filter-trap assay as in (A). Aggregation was performed with 3 μM GST-myc-Htt53Q in the presence of ATP and 0–3 μM TRiC, as indicated. Data were quantified by densitometry. Error bars indicate average ±SD of three experiments.

(C) Electron microscopy of Htt53Q fibrils grown in the absence (a) or presence of 1.5 μM (b) or 0.15 μM TRiC (c). Aggregation of 1.5 μM Htt53Q was carried out for 5 hr, and fibrils were pelleted by centrifugation (15 min, 20,000 × g), followed by negative-stain electron microscopy (Muchowski et al., 2000). Scale bar, 100 nm.

(D) Effect of TRiC on Htt aggregation followed by confocal single-particle fluorescence analysis. Alexa 488- and Alexa 633-labeled GST-Htt53Q (1 μM each) were mixed and incubated without and with TRiC (0.5 μM) added either at the start or at 2 or 6 hr into the aggregation reaction (see Experimental Procedures). Samples were withdrawn at the times indicated, diluted 100-fold, and analyzed by FIDA. Mean particle concentration per confocal volume (C) (top) and particle brightness (Q) (bottom) of FRET-positive aggregates were determined by a one-component 1D-FIDA-fit upon excitation at 488 nm.

chaperones in assisting the folding of newly synthesized proteins.

Results

Direct Role of TRiC in Modulating polyQ Aggregation

To determine whether the proposed involvement of TRiC in polyQ aggregation (Nollen et al., 2004) is direct, we performed in vitro experiments with bovine TRiC and a purified exon 1 fragment of Htt containing a pathologically expanded polyQ repeat of 53 Q. Similar N-terminal fragments, generated by proteolysis from full-length Htt (~350 kDa), were detected in HD brain tissue (Lunkes et al., 2002). Htt53Q was produced as a soluble GST fusion protein cleavable in the linker region between Htt and GST by PreScission protease (PP) (Figure 1A). Cleavage of GST-Htt53Q at concentrations of 1–6 μM resulted in the formation of large, SDS-insoluble aggregates within hours, which were detectable by membrane filtration through a 200 nm pore-sized membrane (Scherzinger et al., 1997). An equimolar concentration of TRiC relative to Htt53Q efficiently inhibited the formation of these aggregates, and partially reduced aggregation was measured at substoichiometric TRiC levels (Figures 1A and 1B). This effect was equally observed in the presence of ATP and in the absence of nucleotide (apyrase treatment) (Figure 1A). Aggregation prevention was mildly enhanced in the presence of ADP or the nonhydrolyzable ATP analog AMP-PNP (Figure 1A), which stabilize the acceptor state of the chaperonin for protein substrate (Meyer et al., 2003). These findings suggest that TRiC functions in this reaction by transiently binding the Htt protein with relatively low affinity.

Analysis by negative-stain electron microscopy demonstrated that TRiC blocked the formation of large polyQ fibrils (Muchowski et al., 2000) in favor of shorter fibrillar structures. This effect was dependent on TRiC concentration (Figure 1C). Whereas fibrils ~20 nm in diameter and longer than 500 nm predominated in the absence of chaperonin (Figure 1Ca), TRiC at a molar ratio to Htt of 1:10 produced fibrils of ~7 nm in diameter and 70–100 nm in length (Figure 1Cc). These aggregates were SDS stable and were retained by the filter membrane (Figure 1B). Even shorter structures of 20–50 nm in length accumulated when TRiC was present at a ratio of 1:1 to Htt (Figure 1Cb). Consistent with their elongated, fibril-like morphology, these aggregates were also stable in SDS (data not shown) but were too small to be detected by membrane filtration (Figure 1B).

Confocal single-particle fluorescence analysis (Giese et al., 2005) was employed to investigate the effect of TRiC on Htt aggregation further. GST-Htt molecules labeled with donor (Alexa 488) or acceptor (Alexa 633) fluorophores at a unique N-terminal cysteine (Schaffar et al., 2004) (see Figure 2B) were mixed at an equimolar ratio, and aggregation was initiated by PP cleavage (see Figure S1 in the Supplemental Data available with this article online). The size (brightness) and concentration of FRET-positive particles passing through an ~1 fL detection volume defined by a focused laser beam was determined by fluorescence intensity distribution analysis (FIDA) without interference from nonaggregated monomers (Kask et al., 2000). An increase in particle brightness due to aggregate growth was observed following cleavage of Htt53Q from GST (Figure 1D). Addition of TRiC at a 1:4 molar ratio to Htt did not affect the early phase of Htt aggregation but arrested aggregate growth (Figure 1D, lower panel), with higher TRiC concentrations resulting in smaller aggregates (data not shown). Arrest of aggregate growth occurred during fibril elongation, as the number of aggregate particles remained constant during this phase (Figure 1D, upper panel). TRiC inhibited aggregate growth even when added 2 or 6 hr after initiating aggregation (Figure 1D), in contrast to Hsp70 and Hsp40, which affect the nucleation phase of polyQ aggregation (Muchowski et al., 2000; Schaffar et al., 2004; Wacker et al., 2004).

A direct interaction of TRiC with Htt protein was demonstrated by single-molecule FRET experiments with Alexa 488-labeled Htt53Q (green emission) and Alexa 647-labeled TRiC (red emission) as a donor-acceptor pair. Analysis by scanning for intensely fluorescent particles (SIFT) (Bieschke et al., 2000; Giese et al., 2005) revealed FRET-positive complexes (red emission) when TRiC was added at the beginning of Htt aggregation or after 6 hr (Figures 1E and 1F). Based on their distribution in segments of high donor fluorescence (green), these TRiC-Htt complexes included Htt aggregates varying in size (Figures 1E and 1F). Together, these observations suggest that purified TRiC interferes with polyQ aggregation by blocking or slowing monomer addition to growing fibrils, consistent with the ability of TRiC to recognize nonnative proteins with β sheet structure (Spiess et al., 2004).

TRiC Cooperates with Hsp70/Hsp40 in Generating Soluble polyQ Oligomers

Next, we investigated the possibility that TRiC may cooperate with the Hsp70 system in modulating Htt aggregation. Interestingly, when Hsp70, Hsp40 (Hdj1), TRiC, and ATP were present in aggregation reactions, 80%–90% of total Htt53Q remained soluble upon centrifugation at 20,000 × g up to 8 hr after cleavage of the GST-Htt fusion protein (data not shown and Figure 2A). Size-exclusion chromatography of the supernatant fraction revealed the presence of Htt oligomers of ~500 kDa (440–700 kDa) (Figure 2Aa), as detected by western blotting. Unlike fibrillar Htt protein, this material was fully SDS soluble upon SDS-PAGE (data not shown). The ~500 kDa oligomers only formed in the presence of both chaperone systems and ATP (Figures 2Aa and 2Ad), and remained soluble upon centrifugation for 1 hr at 100,000 × g (data not shown). In contrast, when Hsp70/Hsp40/ATP alone was present during aggregation, a reduced

(E) Interactions between Htt oligomers and TRiC analyzed by single-particle FRET. Alexa 488-labeled Htt53Q (2 μM) and Alexa 647-labeled TRiC (1 μM) were mixed as donor and acceptor, respectively, and excited at 488 nm. Aggregation was stopped after 10 hr by 200-fold dilution, and mixed TRiC-Htt53Q particles were quantified by SIFT. In the absence of TRiC, most of the Htt species are close to the abscissa (Htt emission, green channel only) (left), whereas upon interaction with TRiC, FRET-positive TRiC-Htt complexes distribute in the higher segments (red TRiC emission and green Htt emission combined) (right).

(F) Quantitation of FRET-positive TRiC-Htt complexes with TRiC added at the start or 6 hr into the aggregation reaction, based on data in (E).

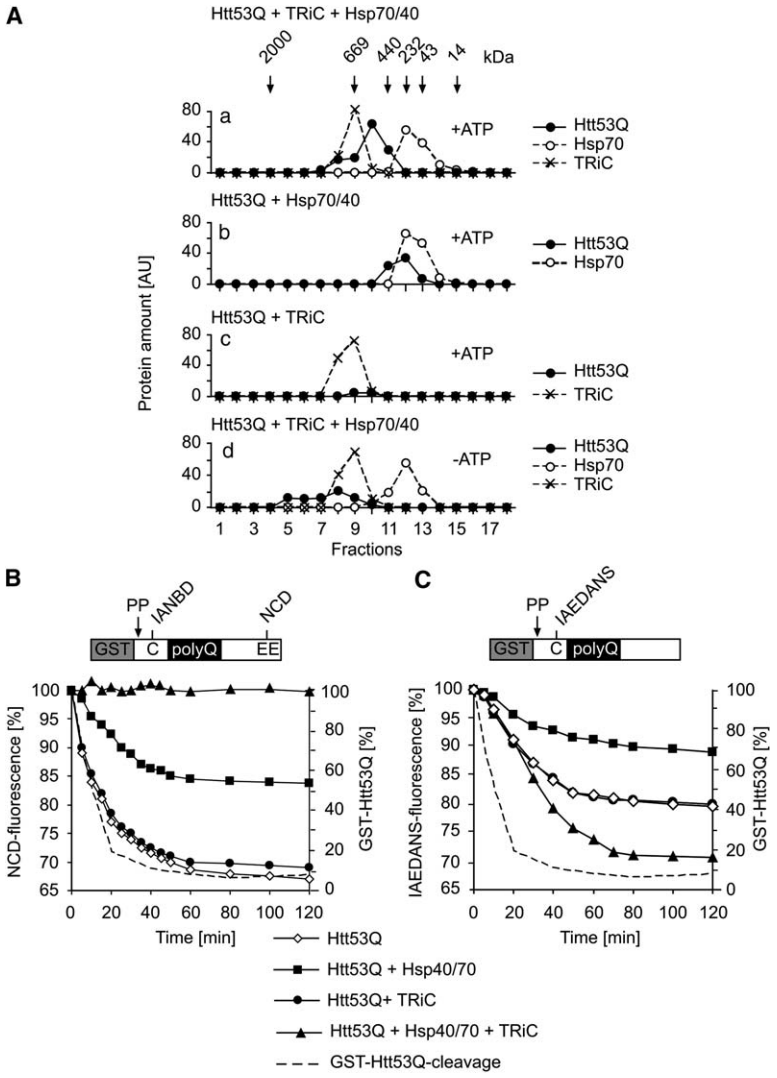

Figure 2. Synergism of Hsp70/Hsp40 and TRiC Activities

(A) Size-exclusion chromatography on a Superose 6 column of the supernatant fraction obtained upon aggregation of Htt53Q (6 μM) for 8 hr in the presence of TRiC, Hsp70 (Hsc70), and Hsp40 (Hdj-1) (6, 12, and 6 μM, respectively) in the combinations indicated. ATP and ATP-regenerating system were present when indicated, and aggregation initiated as in Figure 1A. Fractions were analyzed by immunoblotting with anti-myc (Htt), anti-TRiC, and anti-Hsp70 antibodies and quantified by densitometry. Protein amounts are given in arbitrary units (AU). Positions of molecular weight markers are indicated in kDa. Note that TRiC migrated below its nominal mass of ~900 kDa.

(B) Effects of TRiC (1 μM) and of TRiC, Hsp70, and Hsp40 (0.5, 1, and 0.5 μM) in the presence of ATP as in (A) on intramolecular rearrangements of NCD and IANBD double-labeled Htt53Q upon cleavage of GST-Htt53Q (1 μM) measured by FRET. Kinetics of NCD (donor) fluorescence decrease was monitored at 425 nm. Cleavage of GST-Htt53Q by PP was analyzed in parallel by SDS-PAGE.

(C) Effects of TRiC (1 μM) and of the indicated combinations of TRiC, Hsp70, and Hsp40 (0.2, 1, and 0.5 μM) in the presence of ATP on Htt53Q conformation monitored by changes in IAEDANS fluorescence at 475 nm. Aggregation was performed with 1 μM IAEDANS-labeled GST-Htt53Q (see Experimental Procedures). The kinetics of GST-Htt53Q cleavage from (B) is shown for comparison.

amount of soluble Htt53Q was detected, which partially cofractionated with Hsp70 (Figure 2Ab). Hardly any Htt53Q was recovered from the column with TRiC/ATP alone (Figure 2Ac). The ~500 kDa Htt53Q formed in the presence of both chaperone systems (Figure 2Aa) did not cofractionate with Hsp70 and only partially overlapped with the distribution of TRiC.

Preincubation of aggregating Htt53Q with Hsp70/Hsp40 for 3 hr followed by addition of TRiC for 5 hr resulted in the efficient production of ~500 kDa Htt53Q oligomers, whereas such oligomers were essentially absent when the order of chaperone addition was reversed (Figure S2). These findings suggest that Hsp70/Hsp40 stabilizes monomers or small oligomers of Htt53Q in a conformation competent for subsequent interaction with TRiC, which then mediates formation of the ~500 kDa species. An additional function of Hsp70/Hsp40 downstream of TRiC is also possible.

To monitor conformational changes within Htt53Q associated with the nucleation of oligomer formation, intramolecular FRET experiments were performed with Htt molecules carrying NCD and IANBD dyes as a fluorescence donor-acceptor pair for short-range interactions up to 27–30 Å (Schaffar et al., 2004). IANBD was attached to the N-terminal cysteine and NCD to one of two adjacent glutamates (residues 115 and 116) near the C terminus of Htt53Q (Figure 2B). A time-dependent decrease in donor fluorescence occurred immediately upon cleavage of GST-Htt53Q with PP (Figure 2B) (Schaffar et al., 2004). This decrease in donor fluorescence was only observed when Htt53Q was double labeled with donor and acceptor and thus was due to FRET (Figure S3). Energy transfer was not measurable upon mixing single-labeled molecule populations carrying either donor or acceptor, confirming that the FRET effect observed with double-labeled Htt53Q reflected an intramolecular collapse of the molecules (data not shown; Schaffar et al., 2004). Hsp70/Hsp40 in the presence of ATP partially reduced this conformational compaction. In contrast, TRiC was without detectable effect (Figure 2B). However, Hsp70/Hsp40 and TRiC in combination completely inhibited the collapse of Htt53Q, leading to FRET (Figure 2B). This finding further supports the conclusion that Htt53Q monomers (or small oligomers) become substrates of TRiC following their interaction with Hsp70/Hsp40.

To compare the conformational properties of early Htt oligomers formed with and without chaperones, Htt53Q

was labeled at its unique cysteine with the environmentally sensitive fluorescent probe IAEDANS. An ~20% decrease in IAEDANS fluorescence and a 12 nm red-shift in emission maximum was observed within 60 min upon cleavage of GST-Htt53Q, suggesting increased solvent exposure of the probe (Figure 2C and data not shown). This change occurred with slower kinetics than the intramolecular compaction measured by FRET and reflected Htt oligomer formation (Schaffar et al., 2004). Again, TRiC alone did not affect the conformational properties of Htt measured by its IAEDANS fluorescence properties. In contrast, Hsp70/Hsp40 partially inhibited both the spectral shift and the decrease in fluorescence intensity. Remarkably, Hsp70/Hsp40 and TRiC in combination caused the opposite effect, a 30% decrease in fluorescence intensity and a 16 nm red-shift, indicating a substantial increase in solvent exposure and environmental polarity of the probe (Figure 2C).

These results demonstrate the sequential and cooperative action of Hsp70/Hsp40 and TRiC in modulating Htt conformation and assembly. While TRiC alone inhibits fibril elongation, both chaperone systems together affect the early phase of polyQ oligomerization, producing soluble Htt oligomers of ~500 kDa. These oligomers are presumably protofibrillar in nature and exhibit conformational properties distinct from those of the polyQ oligomers formed in the absence of chaperones or in the presence of Hsp70/Hsp40 alone.

Impairment of TRiC Function Enhances polyQ Toxicity and Aggregation In Vivo

The effect of TRiC on Htt aggregation was investigated in vivo in the yeast *S. cerevisiae*, an established model system for the analysis of polyQ proteotoxicity (Krobitsch and Lindquist, 2000; Meriin et al., 2002; Schaffar et al., 2004; Willingham et al., 2003). When expressed in wild-type cells, Htt exon 1 protein with 20 Q did not form SDS-resistant aggregates detectable by filter-trap assay (Muchowski et al., 2000) (Figure 3A). Htt45Q, close to the threshold length of polyQ pathology of ~37 Q, formed only small amounts of insoluble aggregates, whereas substantial aggregation was observed with Htt96Q (Figure 3A). In conditionally TRiC-defective *tcp1-2* yeast cells, which are temperature sensitive for growth at 37°C (Ursic et al., 1994), the amount of SDS-insoluble aggregates increased ~2-fold upon expression of Htt45Q and Htt96Q at the semipermissive temperature of 30°C (Figure 3A). Interestingly, immunofluorescence revealed that Htt45Q was diffusely distributed in wild-type cells, while in *tcp1-2* cells, the protein coalesced into large, well-defined cytoplasmic inclusions (Figure 3B). This finding mirrored the observation in *C. elegans* that downregulation of TRiC subunit expression results in enhanced polyQ aggregation (Nollen et al., 2004). Enhanced aggregation was not a secondary consequence of defective tubulin biogenesis, because disruption of the tubulin cytoskeleton is known to inhibit formation of large polyQ inclusions (Muchowski et al., 2002). Thus, TRiC, at normal levels, profoundly modulates the aggregation properties of polyQ expansion proteins.

TRiC was diffusely distributed in the cytoplasm in control cells and upon expression of Htt20Q, but colocalized partially with aggregates of Htt96Q (Figure 3C). SDS-insoluble TRiC was detected in Htt96Q-expressing cells by filter-trap assay, presumably reflecting stable incorporation into the aggregates (Figure 3D). This effect was more pronounced in *tcp1-2* cells. However, ~75% of TRiC remained soluble, arguing against a functionally significant depletion of available chaperonin, at least in wild-type cells (data not shown). Indeed, wild-type yeast tolerated the expression of Htt96Q under standard growth conditions without overt toxicity, but expression of Htt96Q markedly aggravated the growth defect of *tcp1-2* cells at 37°C (Figure 3E), which was rescued by expression of wild-type *TCP1* (Figure 3F). Thus, either the polyQ protein becomes toxic when TRiC function is partially impaired, or relocalization of TRiC to Htt aggregates causes a critical reduction in available TRiC activity in *tcp1-2* cells.

Overexpression of TRiC Suppresses polyQ Aggregation

To test more directly whether TRiC is involved in suppressing aggregation and toxicity of polyQ proteins, a yeast strain overexpressing all eight TRiC subunit genes (*TCP1–TCP8*) under galactose-inducible promoters was constructed. These cells produced 5- to 10-fold higher levels of TRiC without significantly reducing the copper-inducible expression of polyQ constructs (Figure S4). The effect of TRiC overexpression on polyQ protein aggregation was analyzed in wild-type yeast as well as in yeast cells having a reduced amount of cytosolic Hsp70s of the Ssa class (*ssa1Δ/ssa2Δ*) or lacking the noncanonical, ribosome-associated Hsp70s Ssb1p and Ssb2p (*ssb1Δ/ssb2Δ*) (Figure 4A and Figure S4). Increased expression of TRiC in wild-type cells markedly inhibited the formation of SDS-insoluble aggregates of Htt96Q and a Htt103Q-GFP fusion protein (Meriin et al., 2002) (Figure 4A). In *ssa1Δ/ssa2Δ* cells, however, efficient TRiC overexpression failed to reduce Htt aggregation (Figure 4A and data not shown). On the other hand, normal inhibition of Htt aggregation by TRiC was observed in *ssb1Δ/ssb2Δ* cells (Figure 4A). These findings support the conclusion from in vitro analysis that TRiC modulates polyQ aggregation in cooperation with the canonical Hsp70 in the cytosol.

TRiC-dependent inhibition of Htt aggregation in the filter assay was only seen upon overexpression of all TRiC subunits but not of various TRiC subunit combinations (Figure 4B). Interestingly, functional expression of the bacterial chaperonin, GroEL, a distant homolog of TRiC, also failed to reduce the formation of SDS-resistant Htt aggregates (Figure 4B) (Kerner et al., 2005) (see Figure S4). Thus, TRiC appears to interact with certain structural features in substrate proteins that are not recognized by GroEL.

Both Htt96Q and Htt103Q-GFP displayed diffuse cytoplasmic staining in TRiC-overexpressing wild-type yeast (Figure 4C) and were largely recovered in the supernatant fraction of cell extracts (data not shown). Small amounts of polyQ protein could be coimmunoprecipitated with antibodies against various TRiC subunits, confirming a direct, but transient, interaction with the chaperonin (Figure 4D). While no soluble Htt96Q was recovered on size-exclusion chromatography of extracts from wild-type cells, TRiC-overexpressing cells

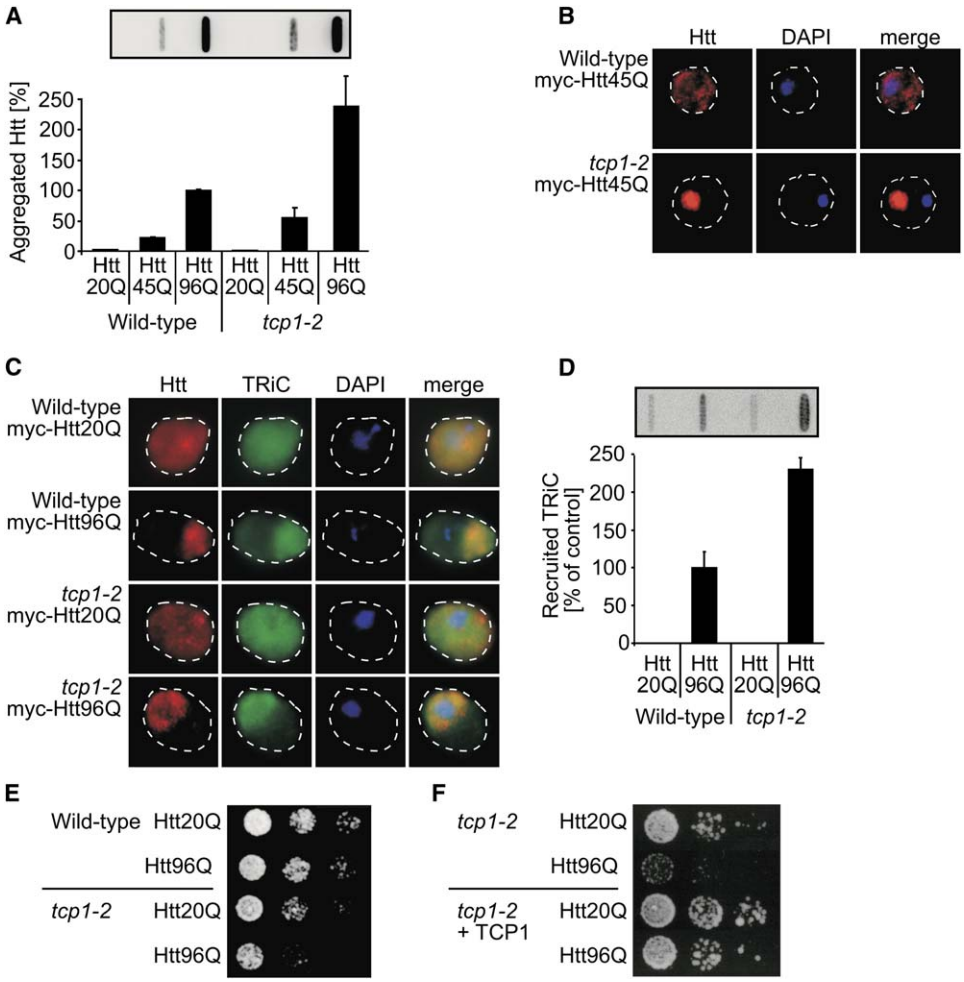

Figure 3. Increased polyQ Toxicity and Aggregation in TRiC-Impaired Yeast

(A) Effect of functional TRiC impairment on Htt aggregation. Myc-tagged Htt exon 1 constructs with 20, 45, and 96 Q were expressed under *CUP1* control for 24 hr in wild-type and *tcp1-2* mutant yeast at 30°C. SDS-resistant aggregates were analyzed by filter assay in cell lysates and detected with anti-myc antibody (see Figure 1A). The amount of Htt96Q aggregates in wild-type cells is set to 100%. Error bars indicate average ±SD of five experiments.

(B) Wild-type and *tcp1-2* mutant cells expressing myc-Htt45Q as above were analyzed by indirect immunofluorescence. myc-Htt45Q was immunolabeled with anti-myc antibody coupled to Cy3-conjugated secondary antibody, and nuclei were counterstained with DAPI.

(C) Recruitment of TRiC subunits into Htt aggregates. Cells were grown and analyzed as in (B). TRiC was immunostained with anti-Tcp5p antibody coupled to FITC-conjugated secondary antibody. Similar results were obtained with anti-Tcp1p antibody (data not shown).

(D) Endogenous TRiC subunit *TCP2* was functionally replaced by C-terminally HA-tagged *TCP2* in wild-type and *tcp1-2* mutant yeast. The filter assay was performed as above, and SDS-resistant aggregates containing Tcp2p-HA were detected with anti-HA antibody. Nonspecific interaction of anti-HA antibody with Htt aggregates was excluded. Amounts of aggregated Tcp2p in cells expressing Htt96Q were set to 100%. Error bars indicate average ±SD of five experiments.

(E) Growth defect of *tcp1-2* mutant cells upon expression of Htt constructs. Cells were cultured in liquid media as in (A), and growth was examined by 5-fold serial dilutions on SC plates after 2 days at 37°C (Schaffar et al., 2004).

(F) The growth defect caused by Htt96Q expression in *tcp1-2* yeast is rescued by wild-type *TCP1*. Htt constructs were coexpressed for 24 hr at 30°C together with either empty vector or *TCP1* under its endogenous promoter, and growth of yeast cells was monitored as in (E).

contained large amounts of Htt96Q that fractionated around 440 kDa (Figure 4E). This material remained fully soluble upon centrifugation at 100,000 × g for 1 hr and was composed of SDS-soluble polyQ protein (data not shown), resembling the properties of the Htt53Q oligomers formed in the presence of TRiC and Hsp70/Hsp40 in vitro (Figure 2A). The distribution of TRiC and of cytosolic Hsp70 (Ssa proteins) was distinct from that of the polyQ oligomers, suggesting that the Htt oligomers formed are no longer efficiently recognized by the ATP-dependent chaperones.

TRiC Prevents Formation of ~200 kDa polyQ Oligomers Correlating with Toxicity

Htt103Q-GFP, unlike Htt96Q, is known to cause a polyQ-length-dependent growth defect of yeast cells (Meriin et al., 2002) (Figure 5A). This proteotoxic effect is dependent on the prion state of Rnq1, which is indicated by the insolubility of Rnq1 protein (Sondheimer and Lindquist, 2000). Overexpression of TRiC efficiently suppressed the growth defect caused by Htt103Q-GFP (Figure 5A) without affecting Rnq1p insolubility (data not shown). In contrast, ~3-fold overexpression of Ssa1p and its

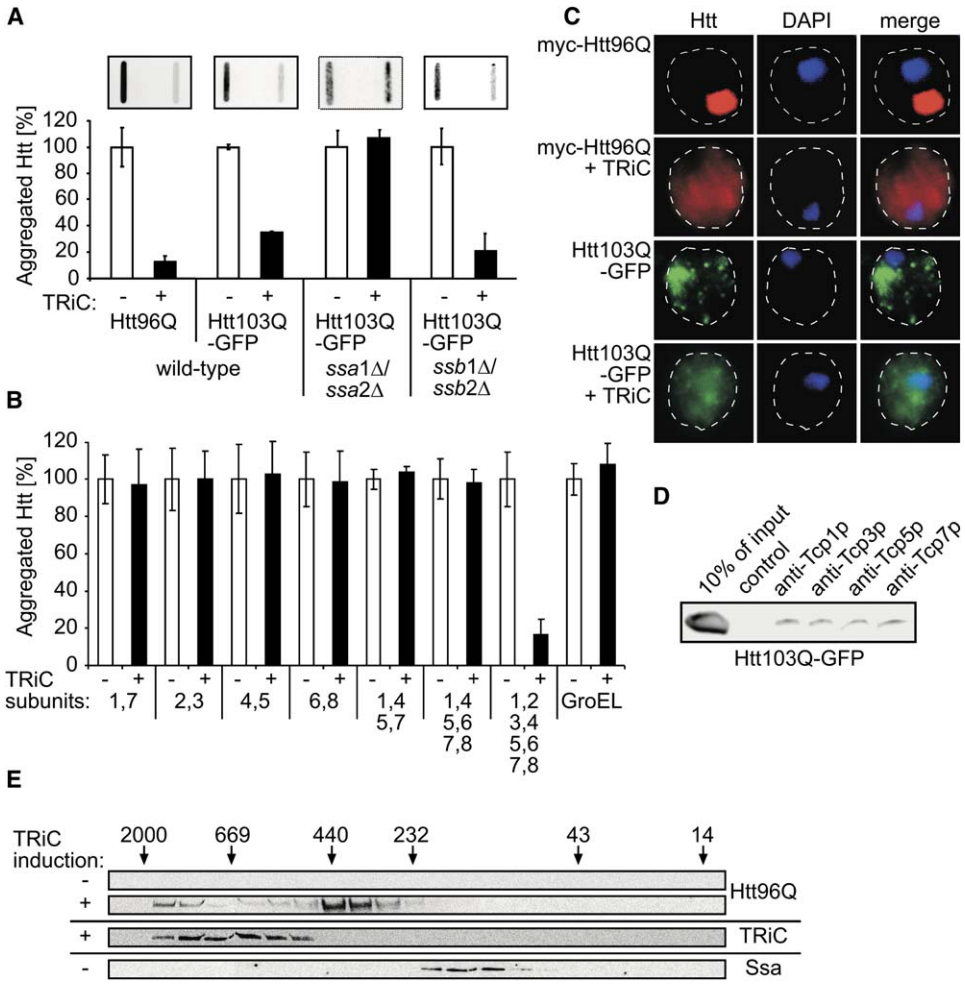

Figure 4. Suppression of Htt Toxicity and Inclusion Formation by TRiC

(A) Effect of TRiC overexpression on Htt aggregation. myc-Htt96Q and Htt103Q-GFP constructs were expressed in wild-type, *ssa1Δ/ssa2Δ*, and *ssb1Δ/ssb2Δ* yeast cells for 24 hr as in Figure 3, with and without overexpression of all eight TRiC subunits from galactose-inducible promoters (see Figure S4). SDS-insoluble Htt aggregates were analyzed by filter assay. Htt103Q-GFP was detected with anti-GFP antibody. Amounts of Htt aggregates without TRiC overexpression were set to 100%. Error bars indicate average ±SD of four experiments.

(B) Effect of overexpression of the various TRiC subunit combinations indicated and of *E. coli* GroEL on Htt96Q aggregation measured as in (A) (see Figure S4). Error bars indicate average ±SD of four experiments.

(C) Cells expressing myc-Htt96Q or Htt103Q-GFP with and without TRiC overexpression as in (A) were analyzed by indirect immunofluorescence with anti-myc antibody and by GFP fluorescence, respectively.

(D) Coimmunoprecipitation of Ht103Q-GFP from soluble lysates of cells overexpressing TRiC (30 min, 20,000 × g) with antibodies against Tcp1p, Tcp3p, Tcp5p, and Tcp7p or control antibody. Precipitates were immunoblotted with anti-GFP antibody. Ten percent of input is shown for comparison.

(E) Size-exclusion chromatography on a Superdex 200 column of soluble fractions from cells expressing Htt96Q in the absence and presence of TRiC overexpression. Htt96Q was detected by immunoblotting with anti-myc antibody and TRiC and Ssa protein with anti-Tcp5p and anti-Ssa antibody, respectively.

Hsp40 cochaperone, Ydj1p, did not rescue the growth defect (Figure 5A and Figure S4), consistent with TRiC being limiting in suppressing polyQ toxicity. On the other hand, overexpression of TRiC in *ssa1Δ/ssa2Δ* cells failed to suppress the growth defect caused by Htt103Q-GFP (data not shown), supporting the conclusion that both chaperone systems must cooperate to alleviate polyQ proteotoxicity in the yeast system.

Interestingly, size-exclusion chromatography of extracts from cells with normal TRiC levels revealed the presence of Htt103Q-GFP oligomers of ~200 kDa (100–230 kDa) (Figure 5B), which were not populated upon expression of Htt96Q (Figure 4E). These Htt103Q-GFP oligomers remained soluble upon centrifugation at 100,000 × g and were readily dissociated by SDS (Figure 5B and data not shown). They partially cofractionated with the Ssa Hsp70 chaperones but could not be coimmunoprecipitated with anti-Ssa antibody (data not shown). Importantly, overexpression of TRiC prevented the formation of ~200 kDa Htt103Q-GFP and produced an increased amount of ~500 kDa Htt103Q-GFP (Figure 5B), comparable to the oligomers of Htt96Q formed upon TRiC overexpression (Figure 4E). A minor amount of unassembled Htt103Q-GFP was detected at ~50 kDa (Figure 5B). Overexpression of Ssa1p/Ydj1p at normal TRiC levels did not prevent the formation of ~200 kDa oligomers (Figure 5B), in line with the failure of Saa1p/Ydj1p to rescue the growth defect caused by

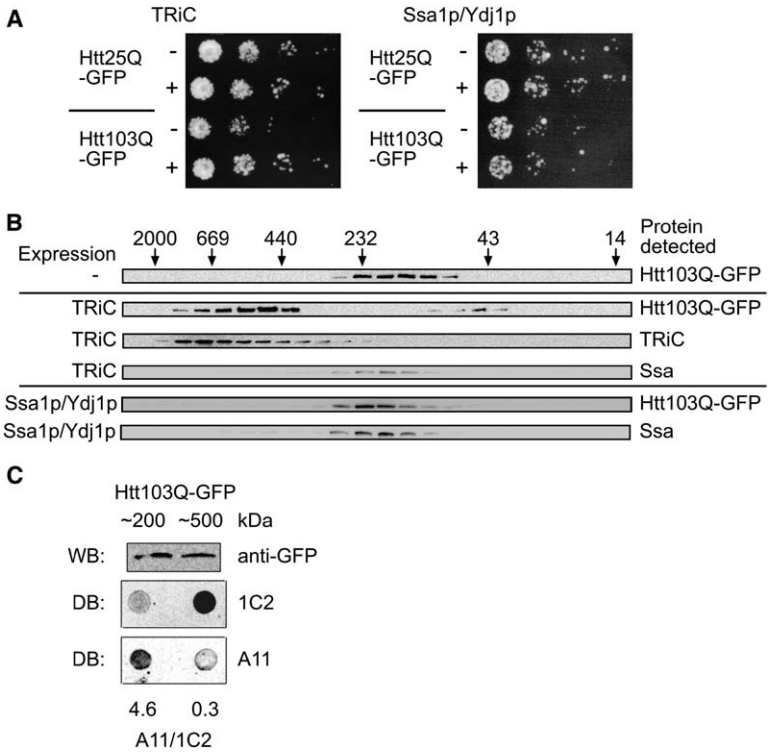

Figure 5. Effects of TRiC and Ssa1p/Ydj1p Overexpression on polyQ Toxicity and Oligomerization

(A) Growth of yeast expressing Htt25Q-GFP or Htt103Q-GFP with and without overexpression of TRiC or Ssa1p/Ydj1p, analyzed as in Figure 3E. For overexpression of chaperones, see Figure S4.

(B) Size-exclusion chromatography as in Figure 4E of soluble fractions from cells expressing Htt103Q-GFP in the absence and presence of TRiC or Ssa1p/Ydj1p overexpression as indicated. Htt103Q-GFP in fractions was detected by immunoblotting with anti-GFP antibody, and chaperone proteins were detected as in Figure 4E.

(C) Analysis of comparable amounts of ~200 and ~500 kDa Htt103Q-GFP oligomers from peak fractions of size-exclusion chromatography in (B) by western blot (WB) with anti-GFP antibody and by dot blot (DB) with antibodies 1C2 and A11. The ratio of A11 to 1C2 signal is given below.

Htt103Q-GFP (Figure 5A). Neither did overexpression of TRiC in *ssa1Δ/ssa2Δ* cells reduce the amount of the ~200 kDa oligomers (data not shown). Thus, presence of these oligomers correlates closely with proteotoxicity under all conditions tested.

A structural differentiation between the ~200 kDa and ~500 kDa Htt103Q-GFP oligomers was achieved based on their immunoreactivity with antibody 1C2, which interacts with an epitope formed by polyQ expansion sequences (Trottier et al., 1995), and antibody A11, which recognizes a sequence-independent structural feature common to soluble amyloid oligomers associated with toxicity (Kayed et al., 2003). Comparable amounts of the two oligomers obtained by size-exclusion chromatography (Figure 5B) were analyzed, as determined by western blotting with anti-GFP antibody (Figure 5C). Dot blot analysis in the absence of SDS showed that the fraction containing the ~200 kDa oligomers was highly reactive with A11 antibody but reacted only weakly with antibody 1C2 (Figure 5C). A11 reactivity was only detected in column fractions when ~200 kDa Htt103Q-GFP oligomers were present (Figure S5). In contrast, the ~500 kDa oligomers were efficiently recognized by antibody 1C2 but essentially lacked A11 reactivity (Figure 5C). Thus, the two types of oligomer are clearly distinct with regard to the conformational properties of the polyQ repeat. Moreover, reactivity with the generic amyloid oligomer antibody A11 would support the view that the ~200 kDa Htt103Q-GFP species is cytotoxic.

Discussion

We have presented evidence that the cytosolic chaperonin TRiC/CCT can interfere with the toxic aggregation pathway of polyQ expansion proteins at different levels (Figure 6). As shown in vitro, TRiC alone does not efficiently inhibit nucleation of aggregation but rather slows the growth of fibrillar aggregates of Htt53Q exon 1, resulting in the accumulation of short, detergent-resistant fibrils. In contrast, in the presence of Hsp70/Hsp40, TRiC affects aggregation early in the pathway by acting on Htt monomers or small oligomers. This cooperative chaperone activity inhibits formation of toxic polyQ species and promotes the assembly of soluble polyQ oligomers of 400–500 kDa without detectable cytotoxicity (Figure 6). These results suggest that the mechanistic principles of chaperone cooperation between Hsp70 and TRiC employed in the pathway of de novo protein folding are also utilized in the cellular defense against potentially toxic, amyloidogenic proteins.

Role of TRiC in Modulating polyQ Protein Aggregation

Several studies have demonstrated an important role of the Hsp70/Hsp40 system in modulating polyQ aggregation and cytotoxicity (see Introduction for references). We demonstrated that the chaperonin TRiC cooperates with Hsp70 in this capacity and may be a limiting factor in suppressing polyQ toxicity. The interaction of Hsp70/Hsp40 and TRiC with polyQ-expanded proteins resembles the sequential action of these chaperones in de novo folding of a subset of cytosolic proteins. In both reactions, the more abundant Hsp70 stabilizes the substrate protein in a conformation that is appropriate for productive interaction with the chaperonin, which then promotes folding to the native state. In both processes, the chaperones act early in the folding/assembly pathway, either on nascent polypeptide chains or on aggregation-prone conformers during incipient polyQ protein aggregation, which may be produced by proteolytic

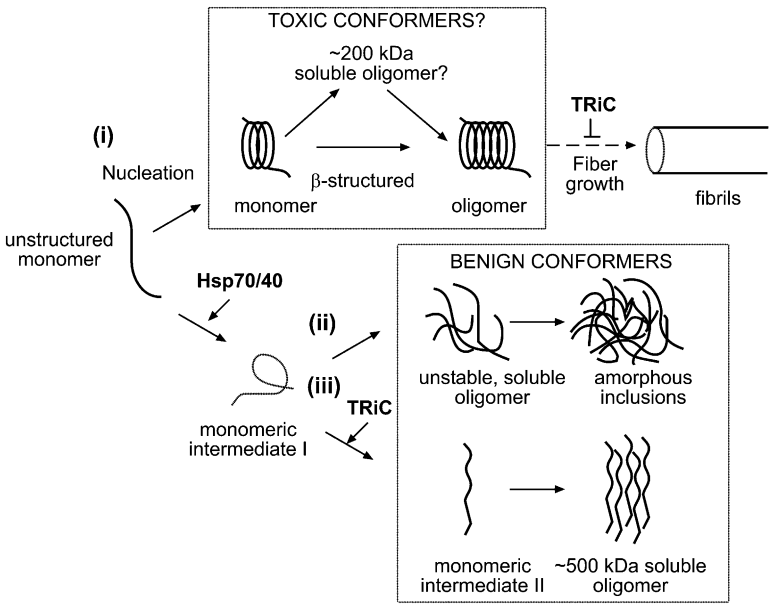

Figure 6. Working Model for the Effects of Hsp70/40 and TRiC on polyQ Protein Aggregation

Nucleation of aggregation is thought to occur at the level of polyQ-expanded monomers of the Htt exon 1 fragment. Early oligomers include prefibrillar forms with cytotoxic properties, such as the oligomers of ~200 kDa that are reactive with A11 anti-oligomer antibody. These oligomers may be off pathway with regard to fibril formation. (i) Reaction with TRiC alone, leading to short polyQ fibrils but not preventing the accumulation of potentially toxic forms; (ii) with Hsp70/Hsp40, favoring the formation of amorphous aggregates; and (iii) with Hsp70/Hsp40 and TRiC combined, leading to soluble oligomers of ~500 kDa, not associated with toxicity and not reactive with A11 antibody.

processing of the full-length disease protein (Lunkes et al., 2002).

Based on experiments in vitro, TRiC alone interacts with relatively low affinity and independent of ATP with a variety of polyQ species, including larger aggregates. Its cooperative function with Hsp70, on the other hand, is likely to involve a predominant interaction with polyQ monomers, presumably followed by their transient, ATP-regulated enclosure in the TRiC central cavity. Mechanistic insight into the synergistic activity of the two chaperone systems was provided by the analysis of a fluorescence-labeled Htt exon 1 fragment. While TRiC alone was unable to interfere with the conformational collapse of the protein occurring during the nucleation phase of aggregation (Schaffar et al., 2004), TRiC and Hsp70/Hsp40 in combination completely prevented this conformational change, as measured by intramolecular FRET. In this reaction, TRiC may modulate structural properties of Htt by acting on the polyQ segment itself and/or its flanking sequences. The end products of the reaction are presumably "folded" Htt exon 1 monomers that assemble into soluble oligomers of ~500 kDa, reminiscent of the role of TRiC in the folding and assembly of proteins such as actin, tubulin, or the von Hippel-Lindau tumor suppressor (VHL) (Frydman, 2001; Melville et al., 2003). TRiC may also be involved in the de novo folding of proteins with normal polyQ repeats.

Existence of Distinct polyQ Oligomeric States

This study also provided evidence that polyQ disease proteins can access conformationally distinct, soluble oligomer states, which may be on pathway or off pathway with respect to the formation of fibrillar inclusions (Figure 6). Substantial amounts of oligomers of ~200 kDa, correlating with cytotoxicity, accumulated when polyQ-expanded Htt was fused to GFP. Htt oligomers of a similar size were previously found to undergo aberrant interactions with a polyQ-containing transcription factor, TBP, in the nucleus (Schaffar et al., 2004). The sequence context with GFP appears to impose a kinetic block on the path toward fibrillar aggregates, thereby causing such intermediates to accumulate and enhancing toxicity. Based on immunoreactivity with the amyloid oligomer antibody A11 (Kayed et al., 2003), the ~200 kDa polyQ oligomers may resemble the potentially toxic, prefibrillar states formed by other amyloidogenic disease proteins and peptides. In contrast, the ~500 kDa polyQ oligomers produced by the cooperative action of Hsp70/Hsp40 and TRiC are conformationally distinct (Figure 6). They lack reactivity with the A11 antibody and are not associated with proteotoxicity in the yeast model. Thus, in the ~500 kDa assembly, the polyQ expansion sequence is presumably prevented from adopting structural features enabling aberrant interactions with other cellular proteins. The ability to distinguish polyQ oligomers with different structural and proteotoxic properties should facilitate screens for compounds that specifically target toxic species.

Implications in Neurodegenerative Disease

Failure of the cooperative Hsp70-TRiC pathway to prevent certain proteins from accessing the conformational space compatible with amyloidogenic aggregation may be critical in the onset of polyQ expansion diseases and perhaps other neurodegenerative folding disorders. In fact, this function may be more generally relevant in protein quality control when considering that the ability to form amyloid structures is not an unusual feature of the small number of proteins associated with diseases but instead may be a generic property of polypeptide chains (Stefani and Dobson, 2003). What factors may be responsible for the failure of chaperone defense in neurodegenerative disease? Recent investigations in the *C. elegans* model suggest that the capacity of the stress protein network, which is regulated by the transcription factor HSF1, may decrease as part of the aging program (Morley and Morimoto, 2004), thus favoring accumulation of toxic protein species. Interestingly, the regulation of TRiC and several other chaperones involved in de novo folding differs from that of

stress-inducible Hsp70 members in that it is HSF1 independent (Albanese et al., 2006). It will therefore be important to see how TRiC is regulated and whether the level of functional chaperonin changes during aging.

Experimental Procedures

Expression Constructs, Yeast Strains, and Proteins

Plasmids pSI244-Htt20Q, pSI244-Htt45Q, pSI244-Htt96Q (2 μ, *LEU2*), and pRS317-Htt96Q (*CEN6*, *LYS2*) were used for copper-inducible expression of myc-Htt proteins in *S. cerevisiae*. Htt25Q-GFP and Htt103Q-GFP (Meriin et al., 2002) were subcloned under control of the *CUP1* promoter into pRS317 (*CEN6*, *LYS2*). *TCP1* was cloned under its endogenous promoter into pRS316 (*CEN6*, *URA3*). *TCP1* and *TCP7*, *TCP2* and *TCP3*, *TCP4* and *TCP5* as well as *TCP6* and *TCP8* were each cloned under individual galactose-inducible promoters into pRS424 (2 μ, *TRP1*), pRS426 (2 μ, *URA3*), pRS425 (2 μ, *LEU2*), and pRS423 (2 μ, *HIS3*), respectively (U.M.B. and K.S., unpublished data) (Figure S4). *SSA1* and *YDJ1* as well as *groEL* were also cloned under individual galactose-inducible promoters into pRS426 (2 μ, *URA3*). A chromosomally integrated gene fusion of the HA epitope to the 3′ end of *TCP2* was generated by homologous recombination of PCR-amplified cassettes in wild-type *TCP1* and *tcp1-2* mutant strains (Siegers et al., 2003). YPH499 was used as the parental wild-type strain (*MATa ura3-52 lys2-801 ade2-101 trp1Δ63 his3Δ200 leu2Δ1*) (Sikorski and Hieter, 1989). *SSB1* and *SSB2* as well as *SSA1* and *SSA2* genes were deleted in strain YPH499 using cre-*loxP* cassettes (Siegers et al., 2003).

For fluorescent labeling, a mutant version of GST-Htt53Q exon 1(Schaffar et al., 2004) was constructed with all four cysteines of GST substituted by serines. Pig brain Hsp70 (Hsc70) and recombinant human Hdj-1 were purified as described (Muchowski et al., 2000). TRiC was purified from bovine testes (Stemp et al., 2005).

Analysis of polyQ Protein Aggregation In Vitro

SDS-resistant Htt aggregates were detected by filter-trap assay with cleavable GST-Htt53Q at 30°C using a 200 nm pore sized cellulose acetate membrane (Muchowski et al., 2000). Effects of TRiC were routinely analyzed in the presence of 2 mM ATP/5 mM $MgCl_2$ and an ATP-regenerating system (200 μg/ml creatine kinase and 20 mM creatine phosphate). Gel filtration of supernatant fractions from aggregation reactions obtained by centrifugation for 15 min at 20,000 × g was performed on a Superose 6 SMART column, and 100 μl fractions were collected, followed by western blot or dot blot analysis with the antibodies indicated. Western blot analysis was used to detect SDS-soluble aggregates.

Intramolecular conformational changes in Htt53Q upon initiation of aggregation by cleavage of GST-Htt53Q were measured by FRET using NCD-4 and IANBD ester (Molecular Probes) as donor-acceptor pair (Schaffar et al., 2004). Labeling with NCD-4 occurred at one of two adjacent glutamates (E115 and E116) of Htt, and IANBD was coupled to the unique cysteine of Htt53Q preceding the polyQ tract (see Schaffar et al. [2004]). Excitation was at 340 nm, and the emission decrease at 425 nm was monitored. Conformational changes in Htt53Q during oligomerization were studied by measuring changes in the environmentally sensitive IAEDANS fluorescence of a singly labeled Htt53Q (Schaffar et al., 2004). Excitation was at 360 nm.

Single-Particle Analysis

Htt53Q used for confocal single-particle analysis was covalently labeled at a unique cysteine residue (Schaffar et al., 2004) with Alexa Fluor 488 C_5-maleimide or Alexa Fluor 633 C_5-maleimide (Molecular Probes). GST-Htt53Q fusion protein (52 μM) was labeled for 3 hr at 4°C in buffer B (50 mM Tris-HCl [pH 8], 150 mM KCl, and 10% glycerol) with a 20-fold molar excess of the dyes added from DMSO. Free dye was removed, and labeling was quantified (Schaffar et al., 2004). The typical GST-Htt53Q:dye ratio was 1:0.5. Confocal single-particle FRET analysis of TRiC-Htt53Q complexes was carried out with Alexa 488-labeled Htt53Q and Alexa 647-labeled TRiC, excited at 488 nm. TRiC (23 μM) was labeled with Alexa Fluor 647 succinimidyl ester (Molecular Probes) for 1 hr at 20°C in 20 mM HEPES-KOH (pH 7.4), 1 mM $MgCl_2$, 100 mM NaCl, 10% glycerol, and 1 mM DTT with a 3-fold molar excess of the dye added from DMSO. Approximately two dye molecules bound per TRiC complex.

SIFT and FIDA measurements were performed on an Insight Reader (Evotec-Technologies, Germany) with either dual-color excitation at 488 nm and 633 nm or with excitation at 488 nm for FRET-based FIDA and SIFT (Bieschke et al., 2000; Giese et al., 2005; Kask et al., 2000). A 40× 1.2 NA microscope objective (Olympus, Japan) and a pinhole diameter of 70 μm at FIDA setting were used. Excitation power was 200 μW at 488 nm and 300 μW at 633 nm. Measurements were for 15 s at room temperature at a scan path length of 100 μm, 50 Hz beamscanner frequency, and 2000 μm positioning table movement (~10 mm/s scanning speed). Data were analyzed using the FCSPP evaluation software version 2.0 (Evotec-Technologies, Germany).

Analysis of polyQ Protein Aggregation in *S. cerevisiae*

Yeast genetic methods, preparation of cell extracts, gel filtration, aggregation assays, and indirect immunofluorecence microscopy were as described (Schaffar et al., 2004; Siegers et al., 2003). PolyQ oligomers were detected by dot blot analysis on nitrocellulose membranes with monoclonal antibody 1C2 (Chemicon International, USA) or polyclonal antibody A11 (Kayed et al., 2003).

Supplemental Data

Supplemental Data include five figures and can be found with this article online at http://www.molecule.org/cgi/content/full/23/6/887/DC1/.

Acknowledgments

The authors thank M. Sherman for the Htt-GFP expression construct, C.G. Glabe for the A11 antibody, E. Craig for anti-Ssa antibodies, W. Baumeister for support with electron microscopy, S. Broadley and M.K. Hayer-Hartl for critically reading the manuscript, and H. Kubota, R. Morimoto, and K. Nagata for exchanging unpublished information. This work was supported by the Deutsche Forschungsgemeinschaft (SFB 596), by the Ernst Jung-Foundation and the German Ministry of Research.

Received: April 21, 2006
Revised: July 7, 2006
Accepted: August 17, 2006
Published: September 14, 2006

References

Albanese, V., Yam, A.Y.W., Baughman, J., Parnot, C., and Frydman, J. (2006). Systems analyses reveal two chaperone networks with distinct functions in eukaryotic cells. Cell *124*, 75–88.

Arrasate, M., Mitra, S., Schweitzer, E.S., Segal, M.R., and Finkbeiner, S. (2004). Inclusion body formation reduces levels of mutant huntingtin and the risk of neuronal death. Nature *431*, 805–810.

Bence, N.F., Sampat, R.M., and Kopito, R.R. (2001). Impairment of the ubiquitin-proteasome system by protein aggregation. Science *292*, 1552–1555.

Bieschke, J., Giese, A., Schulz-Schaeffer, W., Zerr, I., Poser, S., Eigen, M., and Kretzschmar, H. (2000). Ultrasensitive detection of pathological prion protein aggregates by dual-color scanning for intensely fluorescent targets. Proc. Natl. Acad. Sci. USA *97*, 5468–5473.

Chan, H.Y.E., Warrick, J.M., Gray-Board, G.L., Paulson, H.L., and Bonini, N.M. (2000). Mechanisms of chaperone suppression of polyglutamine disease: selectivity, synergy and modulation of protein solubility in Drosophila. Hum. Mol. Genet. *9*, 2811–2820.

Cummings, C.J., Mancini, M.A., Antalffy, B., Defranco, D.B., Orr, H.T., and Zoghbi, H.Y. (1998). Chaperone suppression of aggregation and altered subcellular proteasome localization imply protein misfolding in Sca1. Nat. Genet. *19*, 148–154.

Frydman, J. (2001). Folding of newly translated proteins in vivo: the role of molecular chaperones. Annu. Rev. Biochem. *70*, 603–647.

Giese, A., Bader, B., Bieschke, J., Schaffar, G., Odoy, S., Kahle, P.J., Haass, C., and Kretzschmar, H. (2005). Single particle detection and

characterization of synuclein co-aggregation. Biochem. Biophys. Res. Commun. *333*, 1202–1210.

Hartl, F.U., and Hayer-Hartl, M. (2002). Molecular chaperones in the cytosol: from nascent chain to folded protein. Science *295*, 1852–1858.

Kask, P., Palo, K., Fay, N., Brand, L., Mets, U., Ullmann, D., Jungmann, J., Pschorr, J., and Gall, K. (2000). Two-dimensional fluorescence intensity distribution analysis: theory and applications. Biophys. J. *78*, 1703–1713.

Kayed, R., Head, E., Thompson, J.L., McIntire, T.M., Milton, S.C., Cotman, C.W., and Glabe, C.G. (2003). Common structure of soluble amyloid oligomers implies common mechanism of pathogenesis. Science *300*, 486–489.

Kerner, M.J., Naylor, D.J., Ishihama, Y., Maier, T., Chang, H.C., Stines, A.P., Georgopoulos, C., Frishman, D., Hayer-Hartl, M., Mann, M., and Hartl, F.U. (2005). Proteome-wide analysis of chaperonin-dependent protein folding in *Escherichia coli*. Cell *122*, 209–220.

Krobitsch, S., and Lindquist, S. (2000). Aggregation of huntingtin in yeast varies with the length of the polyglutamine expansion and the expression of chaperone proteins. Proc. Natl. Acad. Sci. USA *97*, 1589–1594.

Landles, C., and Bates, G.P. (2004). Huntingtin and the molecular pathogenesis of Huntington's disease. Fourth in molecular medicine review series. EMBO Rep. *5*, 958–963.

Lunkes, A., Lindenberg, K.S., Ben-Haiem, L., Weber, C., Devys, D., Landwehrmeyer, G.B., Mandel, J.L., and Trottier, Y. (2002). Proteases acting on mutant huntingtin generate cleaved products that differentially build up cytoplasmic and nuclear inclusions. Mol. Cell *10*, 259–269.

Melville, M.W., McClellan, A.J., Meyer, A.S., Darveau, A., and Frydman, J. (2003). The Hsp70 and TRiC/CCT chaperone systems cooperate in vivo to assemble the von Hippel-Lindau tumor suppressor complex. Mol. Cell. Biol. *23*, 3141–3151.

Meriin, A.B., Zhang, X.Q., He, X.W., Newnam, G.P., Chernoff, Y.O., and Sherman, M.Y. (2002). Huntingtin toxicity in yeast model depends on polyglutamine aggregation mediated by a prion-like protein Rnq1. J. Cell Biol. *157*, 997–1004.

Meyer, A.S., Gillespie, J.R., Walther, D., Millet, I.S., Doniach, S., and Frydman, J. (2003). Closing the folding chamber of the eukaryotic chaperonin requires the transition state of ATP hydrolysis. Cell *113*, 369–381.

Morley, J.F., and Morimoto, R.I. (2004). Regulation of longevity in Caenorhabditis elegans by heat shock factor and molecular chaperones. Mol. Biol. Cell *15*, 657–664.

Muchowski, P.J., Schaffar, G., Sittler, A., Wanker, E.E., Hayer-Hartl, M.K., and Hartl, F.U. (2000). Hsp70 and Hsp40 chaperones can inhibit self-assembly of polyglutamine proteins into amyloid-like fibrils. Proc. Natl. Acad. Sci. USA *97*, 7841–7846.

Muchowski, P.J., Ning, K., D'Souza-Schorey, C., and Fields, S. (2002). Requirement of an intact microtubule cytoskeleton for aggregation and inclusion body formation by a mutant huntingtin fragment. Proc. Natl. Acad. Sci. USA *99*, 727–732.

Nollen, E.A.A., Garcia, S.M., van Haaften, G., Kim, S., Chavez, A., Morimoto, R.I., and Plasterk, R.H.A. (2004). Genome-wide RNA interference screen identifies previously undescribed regulators of polyglutamine aggregation. Proc. Natl. Acad. Sci. USA *101*, 6403–6408.

Schaffar, G., Breuer, P., Boteva, R., Behrends, C., Tzvetkov, N., Strippel, N., Sakahira, H., Siegers, K., Hayer-Hartl, M., and Hartl, F.U. (2004). Cellular toxicity of polyglutamine expansion proteins: mechanism of transcription factor deactivation. Mol. Cell *15*, 95–105.

Scherzinger, E., Lurz, R., Turmaine, M., Mangiarini, L., Hollenbach, B., Hasenbank, R., Bates, G.P., Davies, S.W., Lehrach, H., and Wanker, E.E. (1997). Huntingtin-encoded polyglutamine expansions form amyloid-like protein aggregates in vitro and in vivo. Cell *90*, 549–558.

Siegers, K., Bolter, B., Schwarz, J.P., Bottcher, U.M.K., Guha, S., and Hartl, F.U. (2003). TRiC/CCT cooperates with different upstream chaperones in the folding of distinct protein classes. EMBO J. *22*, 5230–5240.

Sikorski, R.S., and Hieter, P. (1989). A system of shuttle vectors and yeast host strains designed for efficient manipulation of DNA in Saccharomyces cerevisiae. Genetics *122*, 19–27.

Sondheimer, N., and Lindquist, S. (2000). Rnq1: an epigenetic modifier of protein function in yeast. Mol. Cell *5*, 163–172.

Spiess, C., Meyer, A.S., Reissmann, S., and Frydman, J. (2004). Mechanism of the eukaryotic chaperonin: protein folding in the chamber of secrets. Trends Cell Biol. *14*, 598–604.

Stefani, M., and Dobson, C.M. (2003). Protein aggregation and aggregate toxicity: new insights into protein folding, misfolding diseases and biological evolution. J. Mol. Med. *81*, 678–699.

Stemp, M.J., Guha, S., Hartl, F.U., and Barral, J.M. (2005). Efficient production of native actin upon translation in a bacterial lysate supplemented with the eukaryotic chaperonin TRiC. Biol. Chem. *386*, 753–757.

Sugars, K.L., and Rubinsztein, D.C. (2003). Transcriptional abnormalities in Huntington disease. Trends Genet. *19*, 233–238.

Trottier, Y., Lutz, Y., Stevanin, G., Imbert, G., Devys, D., Cancel, G., Saudou, F., Weber, C., David, G., Tora, L., et al. (1995). Polyglutamine expansion as a pathological epitope in Huntington's disease and four dominant cerebellar ataxias. Nature *378*, 403–406.

Ursic, D., Sedbrook, J.C., Himmel, K.L., and Culbertson, M.R. (1994). The essential yeast Tcp1 protein affects actin and microtubules. Mol. Biol. Cell *5*, 1065–1080.

Wacker, J.L., Zareie, M.H., Fong, H., Sarikaya, M., and Muchowski, P.J. (2004). Hsp70 and Hsp40 attenuate formation of spherical and annular polyglutamine oligomers by partitioning monomer. Nat. Struct. Mol. Biol. *11*, 1215–1222.

Warrick, J.M., Chan, H.Y.E., Gray-Board, G.L., Chai, Y.H., Paulson, H.L., and Bonini, N.M. (1999). Suppression of polyglutamine-mediated neurodegeneration in Drosophila by the molecular chaperone HSP70. Nat. Genet. *23*, 425–428.

Wetzel, R. (2002). Ideas of order for amyloid fibril structure. Structure *10*, 1031–1036.

Willingham, S., Outeiro, T.F., DeVit, M.J., Lindquist, S.L., and Muchowski, P.J. (2003). Yeast genes that enhance the toxicity of a mutant huntingtin fragment or alpha-synuclein. Science *302*, 1769–1772.

Zoghbi, H.Y., and Orr, H.T. (2000). Glutamine repeats and neurodegeneration. Annu. Rev. Neurosci. *23*, 217–247.